Available online at www.sciencedirect.com
SCIENCE DIRECT®
Bioorganic & Medicinal Chemistry 12 (2004) 3117–3123
Bioorganic & Medicinal Chemistry

The binding of guanine–guanine mismatched DNA to naphthyridine dimer immobilized sensor surfaces: kinetic aspects

Kazuhiko Nakatani,[a,b,*] Akio Kobori,[b] Hiroyuki Kumasawa,[a] Yuki Goto[a] and Isao Saito[a]

[a]*Department of Synthetic Chemistry and Biological Chemistry, Faculty of Engineering, Kyoto University, Kyoto 615-8510, Japan*
[b]*PRESTO, Japan Science and Technology Agency (JST), Kyoto 615-8510, Japan*

Received 15 March 2004; revised 8 April 2004; accepted 8 April 2004
Available online 10 May 2004

Abstract—Naphthyridine dimer composed of two naphthyridine chromophores and a linker connecting them strongly, and selectively, binds to the guanine–guanine mismatch in duplex DNA. The kinetics for the binding of the G–G mismatch to the naphthyridine dimer was investigated by surface plasmon resonance assay. The sensor surface was prepared by immobilizing naphthyridine dimer through a long poly(ethylene oxide) linker with the ligand density of 9.1×10^{-12} fmol nm^{-2}. The kinetic analyses revealed that the binding of the G–G mismatch was sequence dependent on the flanking base pairs, and the G–G mismatches flanking at least one G–C base pair bound to the surface via a two-step process with a 1:1 DNA–ligand stoichiometry. The first association rate constant for the binding of the G–G mismatch in the 5′-CGG-3′/3′-GGC-5′ sequence to the naphthyridine dimer-immobilized sensor surface was 3.2×10^{3} M^{-1} s^{-1} and the first dissociation rate constant was 1.4×10^{-2} s^{-1}. The association and dissociation rate constants for the second step were insensitive to the flanking sequences, and were almost of the same order of magnitude as the first dissociation rate constant. This indicates that the second step had only a small energetic contribution to the binding. The association constant calculated from kinetic parameters was 2.7×10^{5} M^{-1}, which is significantly smaller than the apparent association constants obtained from experiments in solution. Electrospray ionization time-of-flight (ESI-TOF) mass spectrometry on the complex produced from the G–G mismatch and naphthyridine dimer showed the formation of the 1:1 complex and a 1:2 DNA–ligand complex in solution. The latter complex became the dominant complex when a six-fold excess of naphthyridine dimer was added to DNA.

1. Introduction

Heteroduplex analyses[1,2] are the methods that used for the typing of single nucleotide polymorphisms (SNPs) in testing sample DNAs by detecting the mismatched base pairs in heteroduplex produced by strand exchange between sample and the standard DNAs.[3–5] The absence of the mismatched base pairs in a heteroduplex indicated the absence of SNPs in the testing DNAs. Conventional methods for the detection of mismatched base pairs in heteroduplex analyses were enzymatic and chemical cleavage at the mismatched sites,[6–8] gel electrophoresis,[2,9] and selective capture by mismatch-binding proteins.[10,11] We,[12–18] and others,[19–21] have pursued a modified method of heteroduplex analyses for the SNPs detection by using small molecular ligands that can selectively bind to the mismatched base pairs. Molecules binding to the mismatched base pairs in heteroduplex can substitute these low-throughput methods. We have developed novel sensors for a surface plasmon resonance (SPR) assay to detect the G–G,[12] G–A,[17] and C–C[18] mismatch duplexes. The G–G mismatch-detecting sensor was prepared by immobilizing naphthyridine dimer **1**,[12] which strongly and selectively binds to the G–G mismatch.[13] SPR detects the change in the refractive index caused by variation of the mass on the sensor chip surface for example, when the analyte binds to the immobilized ligand on the surface. The change in SPR signal, termed the SPR response presented in resonance units (RU), is directly related to the change in surface concentration of biomolecules. SPR response of 1000 RU is equivalent to the change in surface concentration of 1 ng/mm^2. Thus, the density of immobilized ligands on the surface and amount of analyte bound to the surface could be calculated by the difference in SPR response before and after the analyses. The SPR signal is monitored continuously so that chemical interaction between ligand and DNA can be studied in real time.[22] Naphthyridine dimer **1** (Chart 1) consisted of two 2-amino-7-methyl-1,8-naphthyridines having complementary

Keywords: Mismatch; Kinetics; SPR; Naphthyridine.
* Corresponding author. Tel.: +81-75-383-2756; fax: +81-75-383-2759; e-mail: nakatani@sbchem.kyoto-u.ac.jp

0968-0896/$ - see front matter © 2004 Elsevier Ltd. All rights reserved.
doi:10.1016/j.bmc.2004.04.005

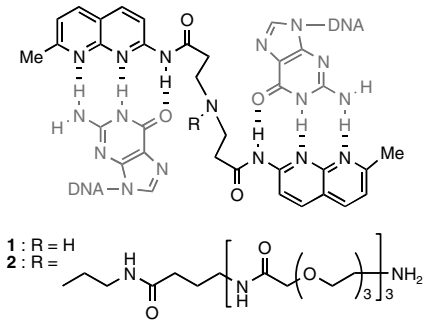

Chart 1. Structures of naphthyridine dimers and their hydrogen bonding to guanines.

surface of hydrogen bonding to a guanine and a linker connecting two chromophores. The sensor surface could differentiate DNA containing the G–G mismatch from that containing normal and other mismatched base pairs.

In addition to the thermodynamic studies, kinetic analysis on the binding of the G–G mismatch to the sensor would provide important information for the molecular design of ligands targeting other mismatched base pairs, and for improving the sensor sensitivity. The density of the ligand immobilized on the surface of SPR sensors significantly affects the sensitivity and the binding kinetics.[23,24] Sensors having a high ligand density on the surface are suitable for the detection of the analyte at low concentrations, whereas those having a low number of ligands on the surface are recommended for kinetic analysis. With the sensor surfaces that had a high ligand density, most of the analyte in the solution was bound to the surface, which increased the sensitivity of the sensor. However, under these conditions, the degree of binding was probably controlled by the rate of mass transport of the analyte from the bulk solution to the surface. This phenomenon, known as mass transport limitation, yields incorrect kinetic parameters for ligand–analyte binding.[25–28] It is also conceivable that, for the sensor surface with a high ligand density, the binding of the analyte to the surface may involve more than one ligand, which would result in complex binding kinetics. In this paper, we have examined the kinetics of the binding of the G–G mismatch duplex to the surface with regard to a different sequence flanking to the mismatch. The kinetic analyses revealed that (1) the binding of the G–G mismatch was found sequence dependent on the flanking base pairs, (2) the G–G mismatches flanking at least one G–C base pair bind to the surface via a two-step process with a 1:1 DNA–ligand stoichiometry, (3) the first association rate constant largely determines the over all efficiency of the binding, and (4) at an excess of ligand concentration a complex with a 1:2 DNA–ligand ratio became predominant.

2. Results and discussion

2.1. Preparation of naphthyridine dimer immobilized sensor surfaces

Naphthyridine dimer **2** tethered to a long poly(ethylene oxide) (PEO) linker was immobilized on an activated

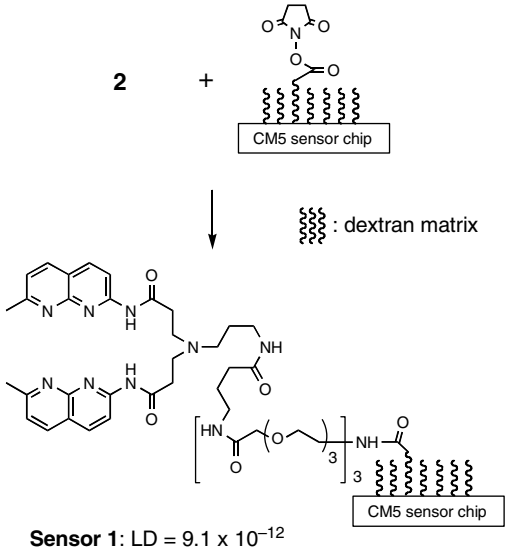

Scheme 1. Synthesis of naphthyridine dimer immobilized sensors. (LD, fmol nm^{-2}).

carboxyl terminal attached to the dextran surface according to the procedure recommended by Biacore (Scheme 1).[29] Immobilization of **1** to the SPR sensor through a long PEO linker was found to significantly increase the SPR intensity.[30] Thus, a 1 mM solution of **2** having a primary amino group at the linker termini in 10 mM of a borate buffer (pH = 9.2) was applied to the carboxylic acid of the CM5 sensor chip activated with *N*-hydroxysuccinimide and EDCI. The degree of immobilization of the ligands was monitored by the increasing SPR signal, and controlled by changing the reaction time. After immobilization of the ligand, the activated esters that remained intact on the surface were destroyed by treating them with ethanolamine. We synthesized a **2**-immobilized sensor surface (**Sensor 1**) by immobilizing **2** for 10 response units (RU). **Sensor 1** had a ligand density on the sensor surface of 9.1×10^{-12} fmol nm^{-2} (1 RU = 1 pg mm^{-2}). Thus, one molecule of **2** existed in an area of ca. 14×14 nm^2 on the surface. Under such an extremely low ligand density, it is reasonable to assume that only one naphthyridine dimer was involved in the binding of the G–G mismatch to the surface.

2.2. Determination of the binding model

Before the kinetic analysis, the binding model of the interaction between the G–G mismatch and **1** was investigated by fitting the sensorgrams to a theoretical binding curve. The 27-mer duplex 5′-d(GTT ACA GAA TCT **XGY** AAG CCT AAT ACG)-3′/3′-d(CAA TGT CTT AGA **X′GY′** TTC GGA TTA TGC)-5′ containing the G–G mismatch (**XGY/X′GY′** = **CGG/GGC**) was applied to **Sensor 1** at DNA concentrations of 2, 5, and 10 μM. All the SPR measurements were carried out at a temperature of 5 °C. The observed sensorgrams were analyzed by a simultaneous curve fitting method for all the sensorgrams and also by an individual curve fitting of each sensorgram using Marquardt–Levenberg

algorithms (Fig. 1).[31] With both methods, it was confirmed that the sensorgrams fit well to a two-state binding model (Eq. 1). However, neither fitted well to simple bimolecular, heterogeneous, nor bivalent binding models. According to the curve fitting by two-state binding model, the SPR response could be resolved into two components, that is, SPR response due to the first state forming (**CGG/GGC−1**)$_A$ from G–G with **1** and the following step producing (**CGG/GGC−1**)$_B$ from (**CGG/GGC−1**)$_A$ (Fig. 2). Because of two-state binding, the fraction of (**CGG/GGC−1**)$_A$ and (**CGG/GGC−1**)$_B$ in the total complex bound to the surface was dependent on the association time. After 90 s of association, the fraction of (**CGG/GGC−1**)$_A$ and (**CGG/GGC−1**)$_B$ were 11.5 and 5.1 RU, whereas it became 12.2 and 9.9 RU after 180 s.

$$\text{CGG/GGC} + \mathbf{1} \underset{k_{d1}}{\overset{k_{a1}}{\rightleftharpoons}} (\text{CGG/GGC}\text{–}\mathbf{1})_A \underset{k_{d2}}{\overset{k_{a2}}{\rightleftharpoons}} (\text{CGG/GGC}\text{–}\mathbf{1})_B \quad (1)$$

To confirm the two-state binding model, the binding of **CGG/GGC** to **Sensor 1** was examined for different

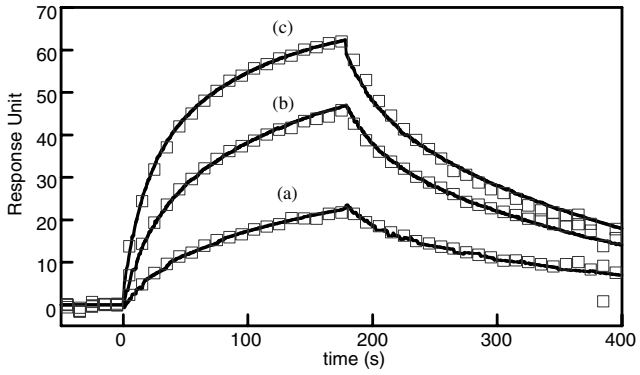

Figure 1. Binding of **CGG/GGC** to **Sensor 1** at different DNA concentrations. Binding was measured for 180 s and dissociation for 220 s. DNA concentration was (a) 2, (b) 5, and (c) 10 μM. Experimental curves (open square) were overlaid with the fitted curves (solid lines) to the two-state model.

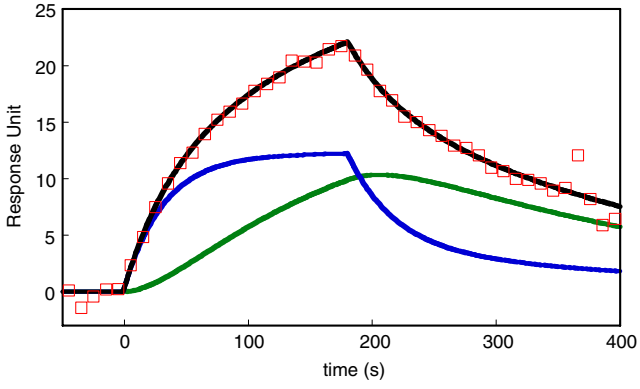

Figure 2. Sensorgram of 2 μM **CGG/GGC** to **Sensor 1**. Shown is the experimental curve (red square) overlaid with the fitted curve (solid black line) from two-state binding model. Simulated curves displaying the initial binding (solid blue line) and subsequence binding (solid green line) are the additive components from the fitted curve.

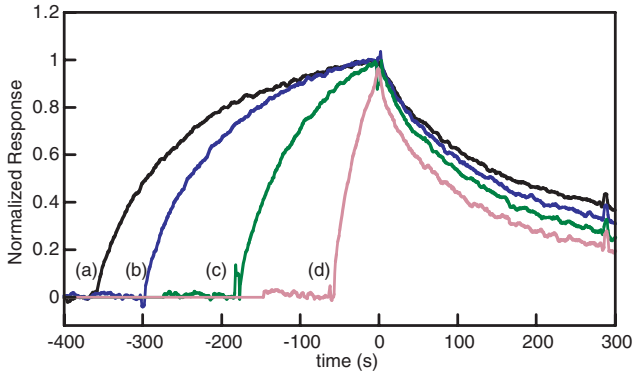

Figure 3. Binding of **CGG/GGC** (2 μM) at different association periods to **Sensor 1**. Association period was (a) 360, (b) 300, (c) 180, and (d) 60 s. Dissociation was measured for 300 s. Response curves were overlaid by zeroing the start of the dissociation phase. Observed responses were normalized by setting the response at the start of the dissociation phase (time = 0 s) to 1.0.

association periods.[24] In the case of simple bimolecular binding, the dissociation curves obtained for different association periods would be superimposable by normalizing the SPR intensity. In contrast, the dissociation curves would not superimpose when the binding involved two states, because the ratio of the two complexes (e.g., (**CGG/GGC−1**)$_A$ and (**CGG/GGC−1**)$_B$) at the initial state of the dissociation phase would be time-dependent on the association phase. As can be seen from Figure 3, the dissociation curves obtained for the association periods of 60, 180, 300, and 360 s showed different dissociation profiles, and were not superimposable on each other. A rapid dissociation was observed with 60 s of association, whereas a much slower dissociation was observed when the G–G mismatch duplex was contacted to the sensor for 360 s. When a bivalent binding (i.e., two molecules of naphthyridine dimer on the surface sequentially bind to the G–G mismatch site) was involved in the interaction between **Sensor 1** and **CGG/GGC**, the dissociation curves were not superimposable. However, bivalent binding was excluded in this particular case, because of the extremely low density of immobilized **2** on **Sensor 1**. On the basis of these experimental results, the binding of the G–G mismatch to **Sensor 1** was concluded to proceed via two states, with the DNA–ligand ratio for the binding being 1:1. While SPR detects the change of the molecular mass on the sensor surface, it has been reported that kinetic analysis can determines the conformational change of the analyte bound on the surface.[32,33] The binding of the G–G mismatch to **Sensor 1** described here is considered as the case.

2.3. Effect of the flanking sequence on the binding kinetics

The kinetics for the binding of the G–G mismatch DNA to **Sensor 1** were investigated regarding the 10 flanking sequences (**XGY/X′GY′**) (Fig. 4). The sensorgrams obtained for the **CGC/GGG**, **TGG/AGC**, **GGC/CGG**, **TGC/AGG**, **AGG/TGC**, **AGC/TGG**, and **AGA/TGT** resembled those of **CGG/GGC** in shape, which validates

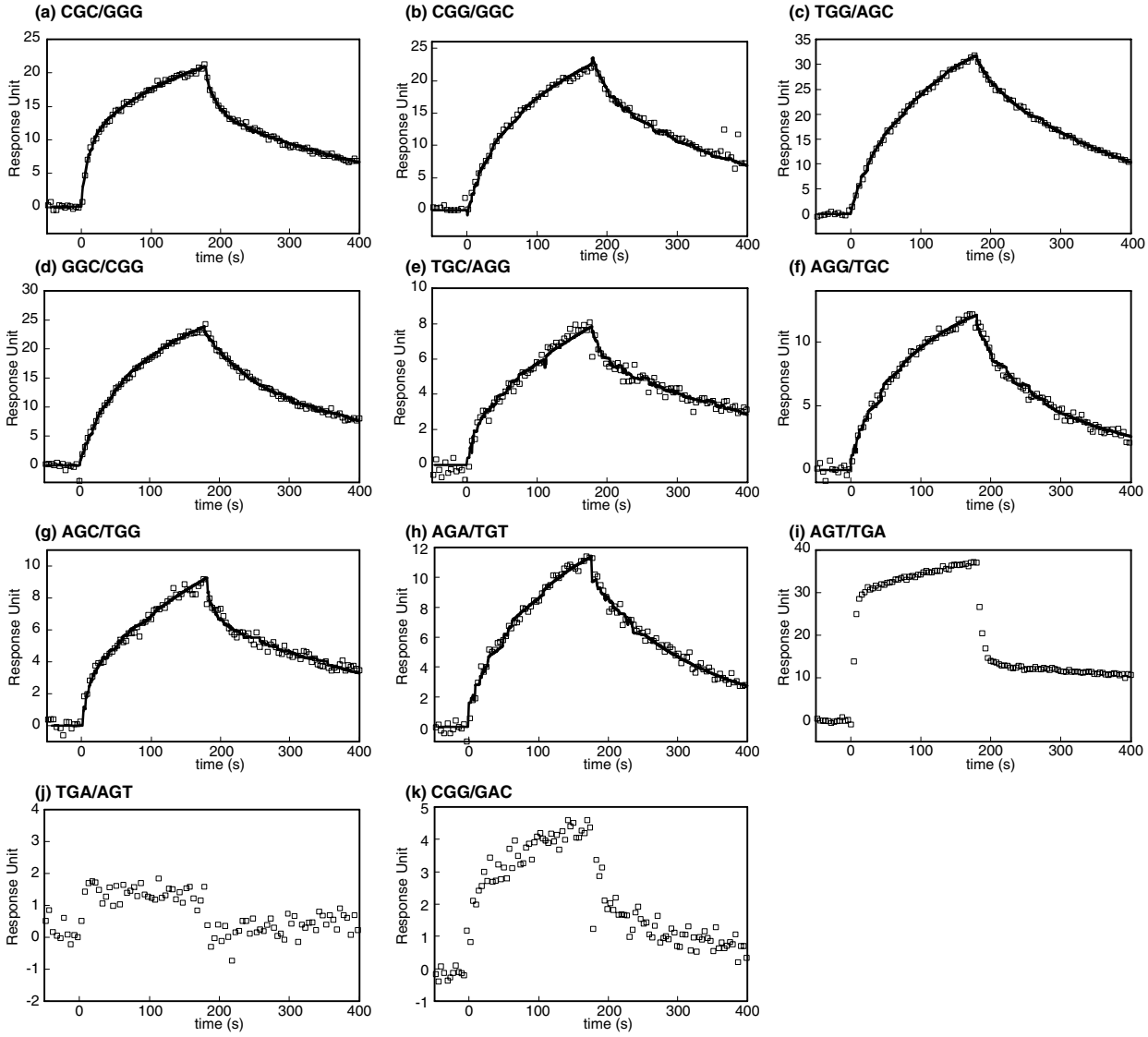

Figure 4. Sensorgrams obtained for the binding of **XGY/X′GY′** to **Sensor 1** at the concentration of 2 μM duplex. Binding was measured for 180 s and dissociation for 220 s. Experimental data (open square) were overlaid with the fitted curve (solid line) to the two-state model except (i), (j), and (k). Key: (a) **CGC/GGG**, (b) **CGG/GGC**, (c) **TGG/AGC**, (d) **GGC/CGG**, (e) **TGC/AGG**, (f) **AGG/TGC**, (g) **AGC/TGG**, (h) **AGA/TGT**, (i) **AGT/TGA**, (j) **TGA/AGT**, (k) **CGG/GAC**.

the analysis of these sensorgrams using a two-state model. In contrast, the sensorgrams obtained for the **AGT/TGA** and **TGA/AGT**, which have A–T base pairs flanking the mismatch, showed a rapid increase and decrease in SPR intensity, and were considerably different in shape from the other sensorgrams. Therefore, analysis using a two-state model was not feasible for these two sequences. It is worth noting that the G–G mismatch in **AGA/TGT**, where one guanine was flanked by two adenines, showed sensorgrams resembling that of **CGG/GGC**, which could be analyzed by using the two-state model.

The kinetic parameters for the eight G–G mismatches were obtained by fitting the sensorgrams at a duplex concentration of 2 μM to the theoretical curve of the two-state model supplied by BIAcore (Table 1). The four kinetic parameters obtained for **CGG/GGC** were $3.2\times10^{3}\ M^{-1}\ s^{-1}$ for the first association rate constant (k_{a1}), $1.4\times10^{-2}\ s^{-1}$ for the first dissociation rate constant (k_{d1}), $0.8\times10^{-2}\ s^{-1}$ for the second association rate constant (k_{a2}), and $6.6\times10^{-3}\ s^{-1}$ for the second dissociation rate constant (k_{d2}). The magnitude of the first association rate constant, k_{a1}, was sequence dependent. The value of k_{d1} was around $10^{-2}\ s^{-1}$, and it did not show any obvious sequence dependence. The rate constants k_{a2} and k_{d2} for the second step were insensitive to the flanking sequences, and were almost of the same order of magnitude as k_{d1}. The equilibrium constant for the second binding step is in the range of 0.4–4 for all G–G mismatches, suggesting that the second step does not directly correlated to the recognition of the G–G mismatches by **1**. The reorganization of the bound DNA duplex on the sensor surfaces is most plausible. These kinetic data suggest that the important binding events involving the intercalation of the naphthyridine chro-

Table 1. Association and dissociation rate constants for the binding of the G–G mismatch duplexes to **Sensor 1**[a]

5′-XYZ-3′ 3′-X′Y′Z′-5′	K_a (M^{-1})	K_{a1} ($M^{-1}\,s^{-1}$)	K_{d1} (s^{-1})	K_{a2} (s^{-1})	K_{d2} (s^{-1})
CGC **GGG**	5.0×10^5	9.4×10^3	5.6×10^{-2}	1.3×10^{-2}	4.4×10^{-3}
CGG **GGC**	2.7×10^5	3.2×10^3	1.4×10^{-2}	0.8×10^{-2}	6.6×10^{-3}
TGG **AGC**	2.5×10^5	2.8×10^3	3.5×10^{-2}	2.8×10^{-2}	8.8×10^{-3}
GGC **CGG**	1.9×10^5	2.5×10^3	1.4×10^{-2}	6.6×10^{-3}	6.1×10^{-3}
TGC **AGG**	1.3×10^5	1.7×10^3	6.0×10^{-2}	2.0×10^{-2}	4.5×10^{-3}
AGG **TGC**	5.1×10^4	1.1×10^3	1.4×10^{-2}	4.9×10^{-3}	7.6×10^{-3}
AGC **TGG**	3.6×10^4	3.9×10^2	4.5×10^{-2}	1.8×10^{-2}	4.5×10^{-3}
AGA **TGT**	3.5×10^4	8.4×10^2	8.7×10^{-3}	4.3×10^{-3}	1.2×10^{-2}
ACT **TGA**	ND[b]	ND	ND	ND	ND
TGA **ACT**	ND	ND	ND	ND	ND
CGG **GAC**	ND	ND	ND	ND	ND

[a] The K_a values were derived from the equation: $K_a = k_{a1}k_{a2}/k_{d1}k_{d2}$.
[b] Not determined due to the inconsistency of the binding model.

mophore onto the mismatched site, the formation of the hydrogen bonds between naphthyridine and the guanine, and a conformational change of the duplex occur in the first step. The magnitude of k_{a1} ranged from $3.9\times10^2\,M^{-1}\,s^{-1}$ for **AGC/TGG**, to $9.4\times10^3\,M^{-1}\,s^{-1}$ for **CGC/GGG**. The value of k_{a1} increased with increasing number of G–C base pairs in the flanking sequence. The G–G mismatches flanking the A–T base pairs were less thermodynamically stable than were those flanking the G–C base pairs.[34] This is rationalized by the improved stacking stabilization of the G–G mismatch by the flanking G–C base pairs compared with the A–T base pairs.[35,36] The observed sequence dependence of k_{a1} may suggest that a partial stacking stabilization of the incoming naphthyridine chromophore into the mismatched site by the flanking G–C base pair(s) accelerates the binding. The G–G mismatches in the **AGT/TGA** and **TGA/AGT** having no G–C base pairs in the flanking sequence would be flexible in structure due to weak stacking stabilization of the mismatched base pair, and susceptible to intercalative binding with the naphthyridine chromophore. The complexes thus formed, however, are not stabilized by stacking with the flanking A–T base pairs, and this results in a rapid dissociation of the complex. The binding of the G–G mismatches flanking the G–C base pairs to the naphthyridine dimer is much slower than that of the G–G mismatches flanking the A–T base pairs. This is most likely due to the greater energy required for the conformational change of the stacked mismatched base pair.

The binding of the G–A mismatch to **Sensor 1** was studied to elucidate the kinetics of the binding of **1** to the G–G mismatch from binding to a nonconsensus mismatch. The SPR signals obtained for the G–A mismatch having two G–C base pairs in the flanking sequence (**CGG/GAC**) were weak, and the shape of the sensorgrams was in-between those of the extremes of **CGG/GGC** and **AGA/TGT**. Therefore, analysis of the sensorgrams using the two-state model was not feasible with **Sensor 1**. While the G–A mismatch in **CGG/GAC** was flanked by two G–C base pairs, the sensorgrams showed a rather rapid association and dissociation. Because the thermodynamic stability of **CGG/GAC** judged from its melting temperature is comparable to that of **CGG/GGC**,[12] the rapid association and dissociation may be attributable to an inconsistency in the surface of the hydrogen bonding between the G–A mismatch site and the naphthyridine dimers.

2.4. Implication for the binding model in solution

The association constant of $K_a = 2.7\times10^5\,M^{-1}$ for **CGG/GGC** calculated from the four kinetic parameters ($K_a = (k_{a1}\cdot k_{a2})/(k_{d1}\cdot k_{d2})$) is significantly smaller than the apparent K_a of $1.9\times10^7\,M^{-1}$ and $9.1\times10^6\,M^{-1}$ obtained in our earlier experiments using DNase I footprint titration and isothermal titration calorimetry (ITC), respectively.[12,14,37] The inconsistency of the results we obtained in these studies using **Sensor 1** with

those obtained in solution is most likely due to a low ligand density of **Sensor 1**, and suggests that a different binding model may be involved in the solution phase. This hypothesis was supported by the observations that the binding of **CGG/GGC** to a **1**-immobilized sensor with an increased ligand density by 50-fold to 4.7×10^{-10} fmol nm^{-2} (cf. 9.1×10^{-12} fmol nm^{-2} for **Sensor 1**) became stronger for all G–G mismatches, but no more fit to 1:1 binding model (data not shown). To gain insight into the binding in solution phase, the complex of the 11-mer duplex 5′-d(CTA ACG GAA TG)-3′/3′-d(GAT TGG CTT AC)-5′ (**cgg/ggc**) containing the G–G mismatch in the sequence of 5′CGG3′/3′GGC5′ and **1** was analyzed by electrospray ionization time of flight mass spectrometry (ESI-TOF MS).[38] When **cgg/ggc** (20 μM) and **1** (20 μM) were mixed in a 1:1 ratio in 100 mM of ammonium acetate in 50% methanol solution, we observed the $[M-5H]^{5-}$ ions corresponding to the 1:1 (**cgg/ggc−1**) and the 1:2 (**cgg/ggc−1·1**) complexes as well as the $[M-5H]^{5-}$ ions of the intact duplex (Fig. 5). The 1:2 DNA–ligand complex became dominant in the mass spectra in the presence of a sixfold excess of **1** in solution. These results suggested that, in addition to the 1:1 binding, a 1:2 binding could also contribute to the high affinity of **1** to the G–G mismatch in solution under a high DNA–ligand ratio (Eq. 2). While the structure of the 1:2 complex discovered in these studies is beyond our knowledge at this moment, the sequence dependence of the SPR intensity obtained by **Sensor 1** may implicate the binding of naphthyridine dimer not only to the G–G mismatch but also to the flanking base pairs.

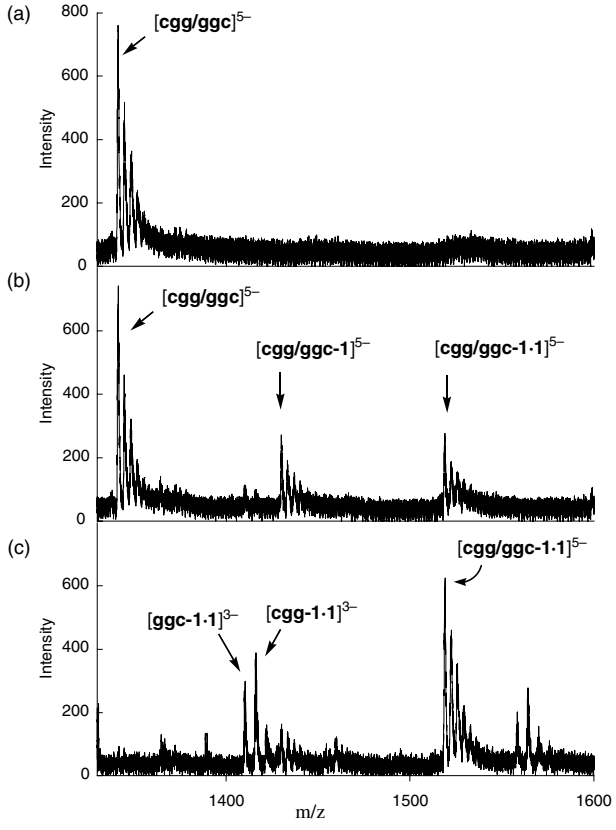

Figure 5. ESI-TOF mass spectra of 11-mer duplex **cgg/ggc** in the absence and presence of **1**. Samples contained 20 μM duplex in 50% aqueous methanol and 100 mM NH_4OAc with **1** at a concentration of (a) 0, (b) 20, and (c) 120 μM. For clarity, the range of m/z from 1330 to 1600 was shown. The ions of the indicated composition accompanied by ions of ammonium adducts.

$$\mathbf{cgg/ggc} + \mathbf{1} \rightleftharpoons \mathbf{cgg/ggc\text{-}1} \overset{\mathbf{1}}{\rightleftharpoons} \mathbf{cgg/ggc\text{-}1{\cdot}1} \quad (2)$$

3. Conclusions

The kinetic analysis of the G–G mismatch to **Sensor 1** confirmed the 1:1 binding. The binding involves two steps, and the efficiency of the binding is governed by the rate of the first binding step of the mismatch to the naphthyridine dimer. In addition to the 1:1 binding, ESI-MS measurements on the complex showed that a bivalent binding mode was also involved in the binding in solution. These observations are important clues for the design of novel ligands that strongly and selectively bind to the mismatched sites.

4. Experimental

4.1. Immobilization of naphthyridine dimer to the surface of SPR sensors

All immobilization were performed in HBS-N running buffer (0.01 M HEPES, pH 7.4, 0.15 M NaCl) using Biacore2000 instrument (Biacore, Uppsala, Sweden) at 25 °C. Naphthyridine dimer **2** was attached to the dextran surface of the sensor chip (CM5, Biacore) following a 10 min activation of surface carboxyl groups using a 1:1 mixture of 1-(3-dimethylaminopropyl)-3-ethylcarbodiimide hydrochloride (EDCI) (1 M) and *N*-hydroxysuccinimide (0.25 M) with a flow rate of 5 μL/min. A 1 mM solution of **2** in 10 mM borate buffer (pH 9.2) was injected until the desired level of response units (RU) had been reached. One flow channel was always left as a blank for a reference. Following attachment, the remaining carboxyl groups on the surface were quenched with 35 μL of 1 M ethanolamine, pH 8.5 with a flow rate of 10 μL/min.

4.2. SPR measurements

SPR measurements were performed in HBS-N running buffer at 4 or 25 °C. Binding was measured for 180 s and dissociation for 220 s before regeneration unless otherwise noted. DNA samples bound on the surface were removed following each measurement by using 7 M urea as regeneration solution at 100 μL/min for 24 min.

4.3. Kinetic analysis of sensorgrams

Response curves used for the fitting were prepared by subtracting the signal generated simultaneously on the flow cell for the control. The response curves obtained for various concentrations of analyte were globally or locally fitted to binding models supplied with the ana-

lytical software of BIA evaluation 3.0. These include simple bimolecular (A + B to AB), heterogeneous (A + B to AB1; A + B2 to AB2), the two-state (A + B to AB then to AB*x*), and a bivalent analyte (A + B to AB and AB + B to ABB) binding models.

4.4. ESI-TOF measurements

ESI-TOF measurements were carried out with JEOL AccuTOF equipment. A solution containing 11-mer duplex containing a mismatch (20 μM) and **1** (20 μM) in 100 mM of ammonium acetate in 50% methanol solution was injected into the ionization chamber.

Acknowledgements

This work was supported by Grant-in-Aid for Scientific Research on Priority Areas (C) 'Medical Genome Science' from the Ministry of Education, Culture, Sports, Science and Technology of Japan.

References and notes

1. Landers, J. P. *Anal. Chem.* **2003**, *75*, 2919–2927.
2. Nataraj, A. J.; Olivos-Glander, I.; Kusukawa, N. *Electrophoresis* **1999**, *20*, 1177–1185.
3. Syvänen, A.-C. *Nat. Rev. Genet.* **2001**, *2*, 930–942.
4. Kwok, P. Y. *Annu. Rev. Genom. Hum. G.* **2001**, *2*, 235–258.
5. Schafer, A. J.; Hawkins, J. R. *Nat. Biotechnol.* **1998**, *16*, 33–39.
6. Myers, R. M.; Larin, Z.; Maniatis, T. *Science* **1985**, *230*, 1242–1246.
7. Rowley, G.; Saad, S.; Giannelli, F.; Green, P. M. *Genomics* **1995**, *30*, 574–582.
8. Roberts, E.; Deeble, V. J.; Woods, C. G.; Taylor, G. R. *Nucliec Acids Res.* **1997**, *25*, 3377–3378.
9. White, M. B.; Carvalho, M.; Derse, D.; O'Brien, S. J.; Dean, M. *Genomics* **1992**, *12*, 301–306.
10. Fazakerley, G. V.; Qignard, E.; Woisard, A.; Guschlbauer, W.; van der Marel, G. A.; van Boom, J. H.; Jones, M.; Radman, M. *EMBO J.* **1986**, *5*, 3697–3703.
11. Smith, J.; Modrich, P. *Proc. Natl. Acad. Sci. U.S.A.* **1996**, *93*, 4374–4379.
12. Nakatani, K.; Sando, S.; Saito, I. *Nat. Biotechnol.* **2001**, *19*, 51–55.
13. Nakatani, K.; Sando, S.; Kumasawa, H.; Kikuchi, J.; Saito, I. *J. Am. Chem. Soc.* **2001**, *123*, 12650–12657.
14. Nakatani, K.; Sando, S.; Saito, I. *Bioorg. Med. Chem.* **2001**, *9*, 2381–2385.
15. Smith, E. A.; Kyo, M.; Kumasawa, H.; Nakatani, K.; Saito, I.; Corn, R. M. *J. Am. Chem. Soc.* **2002**, *124*, 6810–6811.
16. Nakatani, K.; Hagihara, S.; Sando, S.; Sakamoto, S.; Yamaguchi, K.; Maesawa, C.; Saito, I. *J. Am. Chem. Soc.* **2003**, *125*, 662–666.
17. Hagihara, S.; Kumasawa, H.; Goto, Y.; Hayashi, G.; Kobori, A.; Saito, I.; Nakatani, K. *Nucliec Acids Res.* **2004**, *32*, 278–286.
18. Kobori, A.; Horie, S.; Suda, H.; Saito, I.; Nakatani, K. *J. Am. Chem. Soc.* **2004**, *126*, 557–562.
19. Jackson, B. A.; Barton, J. K. *J. Am. Chem. Soc.* **1997**, *119*, 12986–12987.
20. Jackson, B. A.; Alekseyev, V. Y.; Barton, J. K. *Biochemistry* **1999**, *38*, 4655–4662.
21. Lacy, E. R.; Cox, K. K.; Wilson, W. D.; Lee, M. *Nucleic Acids Res.* **2002**, *30*, 1834–1841.
22. Pharmacia-Biosensor. 1990 *Biacore User's Manual.* Piscatway, NJ.
23. Myszka, D. G. *Curr. Opin. Biotechnol.* **1997**, *8*, 50–57.
24. Myszka, D. G.; Wood, S. J.; Biere, A. L. *Methods Enzymol.* **1999**, *309*, 386–402.
25. Glaser, R. W. *Anal. Biochem.* **1993**, *213*, 152–161.
26. Nygren, H.; Werthen, M.; Stenberg, M. *J. Immunol. Methods* **1987**, *101*, 63–71.
27. Stenberg, M.; Nygren, H. *J. Theor. Biol.* **1985**, *113*, 129–140.
28. Bertozzi, C. R.; Bednarski, M. D. *J. Org. Chem.* **1991**, *56*, 4326–4329.
29. Löfås, S.; Johnson, B. *J. Chem. Soc., Chem. Commun.* **1990**, *21*, 1526–1528.
30. Nakatani, K.; Kobori, A.; Kumasawa, H.; Saito, I. *Bioorg. Med. Chem. Lett.* **2004**, *14*, 1105–1108.
31. Morton, T. A.; Myszka, D. G.; Chaiken, I. M. *Anal. Biochem.* **1995**, *227*, 176–185.
32. Sota, H.; Hasegawa, Y.; Iwakura, M. *Anal. Chem.* **1998**, *70*, 2019–2024.
33. Jenkins, J. L.; Lee, M. K.; Valaitis, A. P.; Curtiss, A. C.; Dean, D. H. *J. Biol. Chem.* **2000**, *275*, 14423–14431.
34. Peyret, N.; Seneviratne, P. A.; Allwi, H. T.; SntaLucia, J., Jr. *Biochemistry* **1999**, *38*, 3468–3477.
35. Sponer, J.; Leszczynski, J.; Hobza, P. *J. Phys. Chem.* **1996**, *100*, 5591–5596.
36. Alhambra, C.; Luque, F. J.; Gago, F.; Orozco, M. *J. Phys. Chem.* **1997**, *101*, 3846–3853.
37. It is worth noting that the association constants obtained by DNase I footprint titration assumed a 1:1 binding stoichiometry. Therefore, these were referred as apparent K_a.
38. Beck, J. L.; Colgrave, M. L.; Ralph, S. F.; Sheil, M. M. *Mass Spectrom. Rev.* **2001**, *20*, 61–87.